

Mott Transition v.s. Multicritical Phenomenon of Superconductivity and Antiferromagnetism – Application to κ -(BEDT-TTF)₂X –

Shigeki ONODA^{1*} and Naoto NAGAOSA²

¹*Tokura Spin Superstructure Project, ERATO, Japan Science and Technology Corporation, c/o Department of Applied Physics, University of Tokyo, Hongo 7-3-1, Tokyo 113-8656, Japan*

²*Department of Applied Physics, University of Tokyo, Hongo 7-3-1, Tokyo 113-8656, Japan*

³*Correlated Electron Research Center, AIST, Tsukuba, Ibaraki 305-0046, Japan*

⁴*CREST, Japan Science and Technology Corporation*

(Received February 7, 2020)

Interplay between the Mott transition and the multicritical phenomenon of d -wave superconductivity (SC) and antiferromagnetism (AF) is studied theoretically. We describe the Mott transition, which is analogous to a liquid-gas phase transition, in terms of an Ising-type order parameter η . We reveal possible mean-field phase diagrams produced by this interplay. Renormalization group analysis up to one-loop order gives flows of coupling constants, which in most cases lead to fluctuation-induced first-order phase transitions even when the SO(5)-symmetry exists between the SC and AF. Behavior of various physical quantities around the Mott critical point is predicted. Experiments in κ -(BEDT-TTF)₂X are discussed from this viewpoint.

KEYWORDS: organic superconductivity, Mott transition, antiferromagnetism, renormalization group

Emergence of magnetism and superconductivity (SC) around the Mott transition¹⁾ has been one of the central issues in strongly correlated electron systems. There are two distinct pictures for Mott-insulating states: (I) In Slater’s picture²⁾ justified in the weak correlation limit, the insulating state originates from doubling of a unit cell accompanied by an antiferromagnetic long range ordering. (II) In the Mott-Hubbard picture^{1,3)} valid in the strong correlation limit, the system can be insulating without any symmetry breaking. This insulating feature arises from the Hubbard gap for the charge transfer due to a strong local Coulomb repulsion U . The superexchange interaction between localized spins causes an antiferromagnetic phase transition at a temperature much lower than the Hubbard gap or U . Whether the Mott-Hubbard insulator appears or not depends on the strength of U and magnetic frustrations. Therefore, Mott transitions should be dealt with as a different degrees of freedom from antiferromagnetism (AF).

The dynamical mean field theory (DMFT) has revealed that the Mott transition without any symmetry breaking occurs for the Hubbard model in infinite dimensions.⁴⁾ A first-order Mott transition curve appears by varying a ratio of a bandwidth W to U and terminates at a finite-temperature critical end point (Mott critical point). This Mott transition is analogous to the liquid-gas phase transition, as pointed out in a field theory.⁵⁾ Recently, by restoring spatial correlations neglected in the DMFT, the correlator projection method has given a similar structure of Mott transition in two dimensions but strongly modified by spin correlations.⁶⁾ Diverging compressibility is a common feature at the Mott critical point.^{7,8)}

To describe Mott transitions, one can introduce an Ising-type “order parameter” η with its spatial variations as in the case of lattice gas model. Here, we note that η is not associated with any symmetry breaking. Actually, Kotliar *et al.* have developed Ginzburg-Landau (GL) theory of Mott transition in infinite dimensions where spatial correlations are absent.⁹⁾ For finite-temperature Mott transitions, the order parameter η describes a static eigen mode of the dynamical mean field. Then, to discuss multicritical phenomena of the AF and the SC around the Mott transition, we need to introduce a scalar field η , an O(2) vector field $\vec{\Delta}$ for the SC and an O(3) vector field \vec{m} for the AF.

Layered organic superconductor κ -(BEDT-TTF)₂X offers an ideal laboratory to address this issue. It exhibits a Mott transition as the effective ratio U/W is varied by changing X, isotope effect, and applying pressure.^{10,11)} A phase diagram determined by recent experiments on the Cl salt is summarized in Fig. 1: There exists a first-order Mott transition curve separating SC-AF phases at low temperature, which continues to higher temperature terminating at the Mott critical point $(P_{\text{cr}}, T_{\text{cr}}) \cong (260 \text{ bar}, 40 \text{ K})$.^{11–15)} This Mott critical point has been observed with an anomaly in sound velocity as a diverging charge compressibility κ_{el} ¹³⁾ in agreement with theoretical prediction.^{4,7,8)} This Mott transition appears with a similarity to a liquid-gas phase transition, as in other systems¹⁾ and the theoretical results.^{4–6)}

In this compound, the Neel temperature T_{N} and the superconducting critical temperature T_{c} meet at $(P_{\text{bcr}}, T_{\text{bcr}}) \cong (280 \text{ bar}, 13 \text{ K})$ showing the features of a bicritical phenomenon^{10–12)} (Fig. 1). GL theory for these two competing orders has been proposed,¹⁶⁾ and the analysis of the dynamical critical properties of NMR T_1^{-1} concluded the SO(5) symmetry between the SC and

* E-mail: sonoda@appi.t.u-tokyo.ac.jp

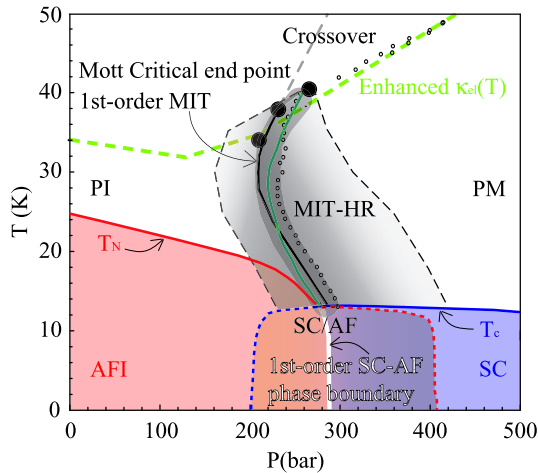


Fig. 1. (Color) Experimental phase diagram of κ -(BEDT-TTF) $_2$ Cu[N(CN) $_2$]Cl with paramagnetic metal (PM), paramagnetic insulator (PI), antiferromagnetic insulator (AFI), inhomogeneously coexistent region of AF and SC (SC/AF), and hysteresis region of metal-insulator transition (MIT-HR). T_c is determined from AC susceptibility χ''^{12} and anomaly in ultrasonic velocity c ,¹³ while T_N from NMR.¹² The first-order SC-AF phase boundary is determined from these three probes.^{12,13} Dotted curves represent spinodal instabilities for metastable AF (red) and SC (blue) determined from NMR,¹² χ' ,¹² and anomaly in c .¹³ The first-order MIT curve is determined from χ' (green solid curve),¹² jump in resistivity ρ (black solid curve)¹⁵ and maximum in $d\rho/dP$ (open circles),¹⁴ all of which lie in the dark shaded region. The MIT-HR is surrounded by spinodal instabilities (black broken curves) determined from hysteresis in ρ .¹⁴ The Mott critical point is the end point (black filled circles for different experiments¹²⁻¹⁵) of the observed first-order MIT curves. Crossover signaled by enhanced charge compressibility (green dashed curve) is determined from dip in c .¹³

AF, which was first proposed for high- T_c cuprates.¹⁷ The SO(5)-symmetric fixed point yields bicritical phenomena where order-disorder phase transitions become second-order. In contrast, away from the SO(5) symmetry, a fluctuation-induced first-order phase transition from disordered to ordered phase¹⁸ or a coexistent phase appears, depending on the strength of competition.

Now, it is highly important to clarify the interplay between Mott transition and the competing two orders, i.e., AF and SC. In this paper, we develop a GL theory for this purpose. Global phase diagram is studied including the fluctuation up to one-loop order. Critical properties around the Mott critical point are also discussed.

We start from the following free energy expansion in terms of three order parameters η , $\vec{\Delta}$ and \vec{m} ;

$$F = \frac{1}{2} \int d\mathbf{r} \left[r_\eta \eta(\mathbf{r})^2 + (\nabla \eta(\mathbf{r}))^2 + \frac{u_{\eta\eta}}{2} \eta(\mathbf{r})^4 - 2h\eta(\mathbf{r}) + r_\Delta \vec{\Delta}(\mathbf{r})^2 + (\nabla \vec{\Delta}(\mathbf{r}))^2 + \frac{u_{\Delta\Delta}}{2} (\vec{\Delta}(\mathbf{r}))^2 + r_m \vec{m}(\mathbf{r})^2 + (\nabla \vec{m}(\mathbf{r}))^2 + \frac{u_{mm}}{2} (\vec{m}(\mathbf{r}))^2 + u_{\Delta m} \vec{m}(\mathbf{r})^2 \vec{\Delta}(\mathbf{r})^2 - (g_\Delta \vec{\Delta}(\mathbf{r})^2 - g_m \vec{m}(\mathbf{r})^2) \eta(\mathbf{r}) \right].$$

h plays a crucial role in describing the Mott critical point as introduced by Kotliar *et al.* in the original arguments of GL theory of Mott transition.⁸ It is expected to obey

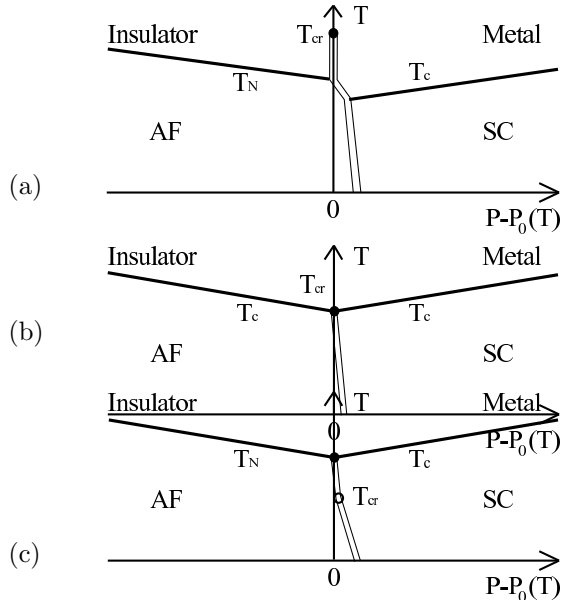


Fig. 2. Schematic MF phase diagrams. Bold and doubled lines represent second-order and first-order transition, respectively, while the circles Mott critical point.

$h \sim h_0(P - P_0(T))$ around the Mott critical point where P controls $(U/W)^{-1}$ and $P_0(T)$ represents its value at the metal-insulator phase boundary. r_i represents a distance from the bare critical point at temperature T_{i0} ($i = \eta, \Delta, m$). It has the form, $r_i \sim a_i(T - T_{i0}(P))$. For SC and AF degrees of freedom, we take into account the effects of P on T_{i0} by expanding it around the Mott critical point as $T_{i0}(P) \sim T_{i0}(P_0(T_{\eta 0})) + b_i(P - P_0(T_{\eta 0}))$ with $b_\Delta > 0$ and $b_m < 0$. u_{ij} ($i, j = \eta, \Delta, m$) describes a quartic coupling constant. g_Δ (g_m) is a lowest-order coupling constant between η and Δ (\vec{m}).

First, we study the mean-field (MF) phase diagrams. If $u_{\Delta m} \gg u_{\Delta\Delta}, u_{mm}$, the coexistence of SC and AF is prohibited. We also restrict ourselves to the case that at $T < T_{cr}, T_c, T_N$, the first-order Mott transition curve separates the SC and the AF with $T_N \geq T_c$. This case is significantly important related to the κ -(BEDT-TTF) $_2$ X system. Then, there are three possibilities as shown in Fig. 2: In (a), the first-order Mott transition runs out above T_c and T_N and ends at a critical point. If $T_{cr} \gg T_c, T_N$, the average $\langle \eta \rangle$ takes $(-)\sqrt{|r_\eta|/u_{\eta\eta}}$ in the metallic (insulating) side. Then, an effective value for $r_\Delta - r_m$ is modified by $(g_\Delta + g_m)\langle \eta \rangle$, which exhibits a jump given by $\delta r_{\Delta-m} = 2(g_\Delta + g_m)\sqrt{|r_\eta|/u_{\eta\eta}}$ at the Mott transition curve. In (b), the bicritical point of SC-AF transition coincides with the Mott critical point. Destiny of this possibility is discussed below using a renormalization group (RG) analysis. In (c), the Mott critical point is inside in the SC-AF phase boundary and η is massive at the bicritical point. Then, the competition between AF and SC becomes the main issue.^{16,17}

Next, we turn to the RG analysis of the fluctuations. We start with the case of Fig. 2 (b), which is crucially modified by the fluctuation into Fig. 3 with the emergence of fluctuation-induced first-order phase transitions. The detailed discussion follows below. Introducing a

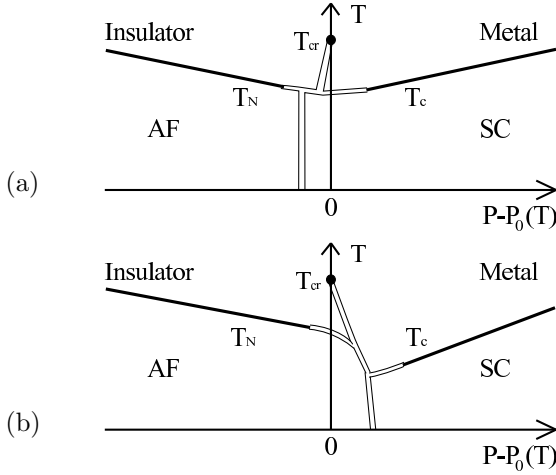


Fig. 3. RG phase diagrams modified by the fluctuations from the MF one given by Fig. 2 (b).

momentum cutoff $\Lambda = e^\lambda$, $\tilde{g}_i \equiv \sqrt{I_d} g_i \Lambda^{-\varepsilon_3}$ and $\tilde{u}_{ij} \equiv I_d u_{ij} \Lambda^{-\varepsilon}$ with the integral $I_d = 2[(4\pi)^{d/2} \Gamma(d/2)]^{-1}$ with $\varepsilon_3 = 3 - \frac{d}{2}$ and $\varepsilon = 4 - d$ (d : the spatial dimension), we obtain the following RG equations for the dimensionless running coupling constants up to one-loop order;

$$\tilde{g}'_\Delta = -\varepsilon_3 \tilde{g}_\Delta + [(N_\Delta + 2)\tilde{g}_\Delta \tilde{u}_{\Delta\Delta} - N_m \tilde{g}_m \tilde{u}_{\Delta m}] - \tilde{g}_\Delta^3 \quad (1)$$

$$\tilde{g}'_m = -\varepsilon_3 \tilde{g}_m + [(N_m + 2)\tilde{g}_m \tilde{u}_{mm} - N_\Delta \tilde{g}_\Delta \tilde{u}_{\Delta m}] - \tilde{g}_m^3 \quad (2)$$

$$\tilde{u}'_{\eta\eta} = -\varepsilon \tilde{u}_{\eta\eta} + 9\tilde{u}_{\eta\eta}^2 + \frac{1}{2}(\tilde{g}_\Delta^4 + \tilde{g}_m^4) \quad (3)$$

$$\tilde{u}'_{\Delta\Delta} = -\varepsilon \tilde{u}_{\Delta\Delta} + [(N_\Delta + 8)\tilde{u}_{\Delta\Delta}^2 + N_m \tilde{u}_{\Delta m}^2] + \tilde{g}_\Delta^4 \quad (4)$$

$$\tilde{u}'_{mm} = -\varepsilon \tilde{u}_{mm} + [(N_m + 8)\tilde{u}_{mm}^2 + N_\Delta \tilde{u}_{\Delta m}^2] + \tilde{g}_m^4 \quad (5)$$

$$\tilde{u}'_{\Delta m} = -\varepsilon \tilde{u}_{\Delta m} + \tilde{g}_\Delta^2 \tilde{g}_m^2 + [(N_\Delta + 2)\tilde{u}_{\Delta\Delta} + (N_m + 2)\tilde{u}_{mm} + 4\tilde{u}_{\Delta m}] \tilde{u}_{\Delta m}, \quad (6)$$

where $N_\Delta = 2$ ($N_m = 3$) is the dimension of $\vec{\Delta}$ (\vec{m}) and $'$ represents a derivative with respect to λ .

When $g_\Delta = g_m = 0$, six fixed points were obtained in terms of ε expansion.¹⁹⁾ Especially, there exist two nontrivial fixed points with nonzero \tilde{u} 's:¹⁶⁾ (A) O(N)-symmetric fixed point $\tilde{u}_{\Delta\Delta} = \tilde{u}_{mm} = \tilde{u}_{\Delta m} = \tilde{u}_{\text{iso}}^*$ with $\tilde{u}_{\text{iso}}^* = \frac{\varepsilon}{N+8}$ and $N = N_\Delta + N_m$. (B) Biconical fixed point $(\tilde{u}_{\Delta\Delta}^*, \tilde{u}_{mm}^*, \tilde{u}_{\Delta m}^*) \approx (0.09048, 0.08475, 0.05358)$ for $d = 3$. In particular, in our case of $N_\Delta = 2$, $N_m = 3$ and $d = 3$, the fixed point (A) is unstable except in a special case $\tilde{u}_{\Delta\Delta} \tilde{u}_{mm} \sim \tilde{u}_{\Delta m}^2$, while (B) is stable.

With $g_\Delta, g_m > 0$, however, there exist no nontrivial stable fixed points, i.e., g_Δ and g_m are relevant couplings at the SO(5)-symmetric fixed point. Fig. 4 shows the RG trajectories of running coupling constants with the SO(5)-symmetric initial condition $\tilde{u}_{\Delta\Delta} = \tilde{u}_{mm} = \tilde{u}_{\Delta m} (= \tilde{u}_0)$ with infinitesimal $\tilde{g}_\Delta = \tilde{g}_m$. \tilde{u} 's stay around \tilde{u}_{iso}^* as long as $\tilde{g}_\Delta, \tilde{g}_m \lesssim 0.5$. ($\tilde{u}_{\Delta m}$ is not shown in Fig. 4, but they behave similarly to \tilde{u}_{mm} .) Therefore it is concluded that as long as $\tilde{g}_\Delta, \tilde{g}_m \lesssim 0.5$, the SO(5)-scaling behavior is observed near the ‘‘bicritical point’’. When $\tilde{g}_\Delta, \tilde{g}_m \gtrsim 0.5$, the instability of the SO(5)-symmetric fixed point is amplified and the bicritical scaling stops. \tilde{u} 's flow to $-\infty$, suggesting the fluctuation-induced first-order transitions.¹⁸⁾ The difference among

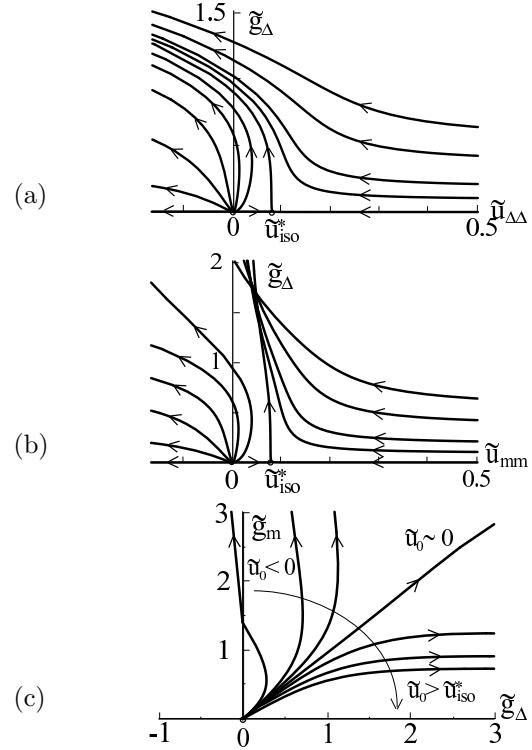


Fig. 4. The RG trajectories around the SO(5)-symmetric fixed point obtained under the initial condition $\tilde{u}_{\Delta\Delta} = \tilde{u}_{mm} = \tilde{u}_{\Delta m} = \tilde{u}_0$ at the scale $\tilde{g}_\Delta = \tilde{g}_m \rightarrow 0$. Curves in (b) correspond to different values for \tilde{u}_0 .

\tilde{u} 's rapidly increases in the run-away trajectories far from the SO(5)-symmetric fixed point (Figs. 4 (a) and (b)), because of the difference between \tilde{g} 's. Trajectories $(\tilde{g}_\Delta, \tilde{g}_m)$ shown in Fig. 4 (c) depend on the initial value of $\tilde{u}_0 = \tilde{u}_{\Delta\Delta} = \tilde{u}_{mm} = \tilde{u}_{\Delta m}$. For the choices of $\tilde{u}_0 > 0$, \tilde{g}_Δ becomes larger than \tilde{g}_m due to the difference of $N_\Delta = 2$ and $N_m = 3$, and $\tilde{u}_{\Delta\Delta}$ turns to be negative faster than \tilde{u}_{mm} and $\tilde{u}_{\Delta m}$. Flows of $\tilde{u}_{\eta\eta}$ are also similar to $\tilde{u}_{\Delta\Delta}$, indicating a first-order Mott transition. These RG results suggest a phase diagram shown in Fig. 3 (a) with the dominant SC over the AF. So far we have considered the RG flows around the SO(5) fixed point. On the other hand, if we consider the coupling constants far from the SO(5) fixed point and take $\tilde{g}_m \gg \tilde{g}_\Delta$, \tilde{g}_m remains to be larger than \tilde{g}_Δ and \tilde{u}_{mm} turns to be negative faster than $\tilde{u}_{\Delta\Delta}$ and $\tilde{u}_{\Delta m}$. Then, there occurs another possibility of phase diagram shown in Fig. 3 (b) with the dominant AF over the SC. A phase diagram with a fluctuation-induced first-order phase transition to a coexistent phase is also possible. To determine which ordered phase appears, we must include higher-order couplings into the free energy and examine the parameters in detail. This is beyond the scope of this paper.

We turn to the cases of MF phase diagrams Fig. 2 (a) and (c). In these cases, the η -field is massive around $(T_{\text{bcr}}, P_{\text{bcr}})$, i.e., $|r_\eta|/\Lambda_0^2 \neq 0$ (Λ_0 is the initial momentum cut-off). (I) When $|r_\eta|/\Lambda_0^2 < 1$, the fluctuation of η is relevant and the RG analysis based on eqs. (1)-(6) applies for $\Lambda_d = \sqrt{|r_\eta|} < \Lambda < \Lambda_0$. If an instability with negative \tilde{u} 's occur before this scaling stops at Λ_d , then the phase diagram is again given by Fig. 3(a) or (b).

Otherwise, the scaling for $\Lambda < \Lambda_d$ crosses over to that in the following case (II). (II) When $|r_\eta|/\Lambda_0^2 > 1$, we can neglect the fluctuations of η , and the problem is reduced to that of $\vec{\Delta}$ and \vec{m} only by putting $\eta = \pm\sqrt{|r_\eta|/u_{\eta\eta}}$ in the case of Fig. 2 (a) and $\eta = 0$ in the case of Fig. 2 (c). Furthermore, in the case of Fig. 2 (a), the discontinuity $\delta r_{\Delta-m}$ of $r_\Delta - r_m$ at the first-order Mott transition produces another scale for a crossover: The RG flows for $\tilde{u}_{\Delta\Delta}$, \tilde{u}_{mm} , and $\tilde{u}_{\Delta m}$ with \tilde{g} 's being zero in eqs. (4)-(6)¹⁶ should be stopped at $\Lambda_c = \sqrt{\delta r_{\Delta-m}}$. Therefore, when $\delta r_{\Delta-m} > \Lambda_0^2$ in Fig. 2 (a), AF and SC are well separated by the first order Mott transition, while the scaling theory in ref.¹⁶ applies for the range of $\Lambda_c < \Lambda < \Lambda_0$ in the case of $\delta r_{\Delta-m} < \Lambda_0^2$.

Now we discuss the phase diagram of κ -(BEDT-TTF)₂X shown in Fig. 1. The Mott critical point is well above T_{bcr} , and the phase diagram looks like Fig. 2 (a). Therefore SC and AF occur independently separated by the first order Mott transition, and do not interact with each other. However T_m and T_Δ almost coincide (within 1 K) at the "bicritical point", and the observed singular behavior of NMR relaxation rate strongly suggests the SO(5) bicritical scaling.¹⁶ These suggest that SC and AF are communicating each other across the Mott transition. This dilemma could be resolved assuming small $\delta r_{\Delta-m}/\Lambda_0^2$ because the bicritical scaling governed by SO(5) fixed point should be observed in a certain region before the coupling to η grows. This small value of $\delta r_{\Delta-m}/\Lambda_0^2$ also leads to fluctuation-induced first-order phase transitions to SC and/or AF, as obtained in the RG analysis (Fig. 3). This is not excluded in Fig. 1, because the first-order Mott transition must be accompanied by a hysteresis region which defines metastabilities of metallic and insulating states. The fluctuation-induced first-order phase transitions to SC and/or AF might be hidden in this hysteresis region, and further experiments on the metastability are required. Moreover, if T_{cr} approaches T_{bcr} in other materials by varying the geometrical frustration,⁶ then the present scenario has a more chance to be observed experimentally.

Lastly, we discuss critical properties around the Mott critical point ($P_{\text{cr}}, T_{\text{cr}}$). The critical properties are described by the Ising universality class. Then, the specific heat, the derivative of $\langle\eta\rangle$ with respect to h and its jump $\delta\langle\eta\rangle$ obey the following scaling laws,

$$C \propto |T - T_{\text{cr}}|^{-\alpha} \quad (7)$$

$$\partial\langle\eta\rangle/\partial h|_{T, h=h_{\text{cr}}} \propto (T - T_{\text{cr}})^{-\gamma} \text{ for } T > T_{\text{cr}}, \quad (8)$$

$$\delta\langle\eta\rangle|_{T, h=h_{\text{cr}}} \propto (T_{\text{cr}} - T)^\beta \text{ for } T < T_{\text{cr}}, \quad (9)$$

$$\delta\langle\eta\rangle|_{T=T_{\text{cr}}, h} \propto |h - h_{\text{cr}}|^{1/\delta} \quad (10)$$

with $\alpha \sim 0.013$, $\gamma \sim 1.25$, $\beta \sim 0.31$ and $\delta \sim 5.0$ in three dimensions.²¹ Here, h_{cr} is the critical value of h and $h_{\text{cr}} = 0$ if we take $\vec{\Delta} = \vec{m} = 0$ in our free energy. We note that the double occupancy D and U play roles of the density and the pressure, respectively, in the analogy to the liquid-gas phase transition.⁴⁻⁶ Therefore D and $\partial D/\partial U$ exhibits the same critical properties as $\langle\eta\rangle$ and $\partial\langle\eta\rangle/\partial h$, and hence the local magnetic moment which is given by $\frac{1}{4} - \frac{D}{2}$ in the Hubbard model. The singularity at the crit-

ical point and the discontinuity at the first-order phase boundary can also be observed in other physical quantities such as resistivity, Drude weight, spin susceptibility, longitudinal and transverse thermal conductivity. It is because these quantities can be expanded in terms of $\langle\eta\rangle/T$ and the first-order term exhibits a dominant singularity. Then, in the vicinity of the Mott critical point, the same scaling properties as η can be observed by replacing h with P . Especially, the thermal Hall conductivity may be useful for the experimental scaling analysis, since phonon contributions are usually negligible.

We have considered only the half-filling case, but one can consider the electron filling n as another controlling parameter in addition to U/W . Especially, the divergence of κ_{el} at the critical point^{7,8} has been observed as an anomaly of the sound velocity c in ultrasonic measurements by Fournier *et al.*,¹³ although it is still difficult to estimate the scaling property from the experiment. The same anomaly for c can also be obtained with Raman scattering experiment. Extension of GL theory including n is an interesting problem left for future studies.

The authors acknowledge K. Kanoda, K. Miyagawa, F. Kagawa for stimulating discussion and providing experimental data before publication. They also thank S. Murakami for fruitful discussion.

-
- 1) N. F. Mott, *Metal-Insulator Transitions*, (Taylor and Francis, London/Philadelphia, 1990).
 - 2) J. C. Slater, Phys. Rev. **82**, 538 (1951).
 - 3) J. Hubbard, Proc. Roy. Soc. A **276**, 238 (1963); *ibid.* **281**, 401 (1964).
 - 4) A. George *et al.*, Rev. Mod. Phys. **68**, 13 (1996).
 - 5) C. Castellani *et al.*, Phys. Rev. Lett. **43**, 1957 (1979).
 - 6) S. Onoda and M. Imada, Phys. Rev. B **67**, R161102 (2003).
 - 7) S. Onoda and M. Imada, J. Phys. Soc. Jpn. **73**, 3998 (2001); unpublished (cond-mat/0304580).
 - 8) G. Kotliar, S. Murthy and M.J. Rozenberg, Phys. Rev. Lett. **89**, 046401 (2002).
 - 9) G. Kotliar, E. Lange and M.J. Rozenberg, Phys. Rev. Lett. **84**, 5180 (2000).
 - 10) H. Ito *et al.*, J. Phys. Soc. Jpn. **65**, 2987 (1996); Y. V. Sushko and K. Andres, Phys. Rev. B **47**, 330 (1993).
 - 11) K. Kanoda, Physica C **282-287**, 299 (1997).
 - 12) S. Lefebvre *et al.*, Phys. Rev. Lett. **85**, 5420 (2000).
 - 13) D. Fournier *et al.*, Phys. Rev. Lett. **90**, 127002 (2003).
 - 14) P. Limelette *et al.*, unpublished (cond-mat/0301478).
 - 15) F. Kagawa, *et al.*, unpublished.
 - 16) S. Murakami and N. Nagaosa, J. Phys. Soc. Jpn. **69**, 2395 (2000). See also S. Murakami and N. Nagaosa, Phys. Rev. Lett. **90**, 197201 (2003).
 - 17) S.-C. Zhang, Science **275**, 1089 (1997).
 - 18) T. Natterman and S. Trimper, J. Phys. A **8**, 2000 (1975); S.A. Brazovskii and I.E. Dzyaloshinskii, Sov. Phys. JETP Lett. **21**, 164 (1975); J. Rudnick, Phys. Rev. B **18**, 1406 (1978).
 - 19) D.R. Nelson, J.M. Kosterlitz and M.E. Fisher, Phys. Rev. Lett. **33**, 813 (1974); J.M. Kosterlitz, D.R. Nelson and M.E. Fisher, Phys. Rev. B **13**, 412 (1974).
 - 20) A. Kawamoto, *et al.*, Phys. Rev. B **52**, 15522 (1995); *ibid.* **55**, 14146 (1997).
 - 21) S.-K. Ma, *Modern Theory of Critical Phenomena*, (Addison-Wesley, 1976)